EVS29 Symposium
Montréal, Québec, Canada, June 19-22, 2016

Real-Time Estimator Li-ion Cells Internal Resistance for Electric Vehicle Application

Alexandre O. Tessier[1], Maxime R. Dubois[1] and João P. Trovão[1]

[1] *e-TESC Laboratory, University of Sherbrooke, J1K 2R1, Québec, Canada,*

{A.Tessier, Maxime.Dubois, Joao.Trovao}@USherbrooke.ca

Short Abstract

Battery Management Systems (BMS) were introduced into Li-ion battery packs to serve several purposes, among which assertion of the small variations of the cells state of charge and increase of their life cycle. This paper offers a complete real-time working model for the on-line measurement of the cells internal resistance, which requires very low computation time and enough precision for electric vehicle applications. Some electric models used for the determination electrical parameters have a huge complexity and are not implementable in automotive processing units. Among many solutions, the proposed approach uses cell modeled as a source-resistance with low complexity, without loss measurement precision, or increase the computation capabilities.

1 Introduction

No actual battery chemistry allows a single cell to meet electric or hybrid vehicle's power demand and energy storage requirements. Hundreds of cells in series and/or parallel are common in modern battery packs. Li-ion and Li-Po chemistries are today's most trusted families for power-capable and light-weighed battery packs. However, using Li-ion or Li-PO for electric vehicle (EV) propulsion comes with one flaw: small differences in the cells capacity and self-discharge current will result in local overcharges and over-discharges after only a few charge-discharge cycles, which, if not asserted, will greatly impede the battery pack lifetime [1], [2]. Furthermore, cell overcharging may result in fire or explosion and other safety issues for the end user.

To lengthen the battery pack life cycle and reduce the risks of failure, a battery management system (BMS) is a necessary add-on to the battery pack for the monitoring and control of the cells behavior. As the accurate chemical reaction is complex, electrical models were created in order to translate some aspects of the chemical reactions in the cells into measurable electrical parameters [3]. Fig. 1 presents a classic electrical model for Li-ion batteries. Typically, the cell behavior can be represented with a voltage source, function of the State-of-Charge (SOC), a complex impedance Z_{in} composed of an ohmic resistance R_{Ω} and a polarization impedance Z_{pol}, which both together represents the cell losses (proportional to i^2), and a leaking resistor R_{leak}, which represents long-term charge loss. R_{in} should actually be expressed as a complex impedance Z_{in}, but for a coherent representation with current literature, it will be denoted as R_{in} in this paper.

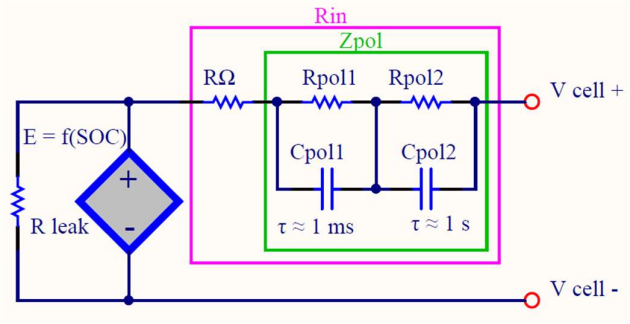

Figure 1: Basic electrical model for a Li-ion cell

A number of researchers have argued that the accuracy of the model described in Fig. 1. Thus, more advanced (and complex) models have been proposed, to describe the cell behavior [4] - [7]. These models often mix electrical, thermal and chemistry considerations in order to achieve high accuracy. Recent studies have also proposed cell modeling including Kalman filters, space-state models, parametrical or complex impedance. Although these models demonstrate accuracy and reliability, never could they be implemented in automotive processors in order to be suitable for low-cost electric or hybrid vehicles designs [8]. These more complex, more advanced models can be implemented for real-time identification of their parameters only off-line on Desktop computers (running at around 3 GHz with 4 to 8 processors in parallel), but cannot be adapted to an on-line measurement of the cell behavior on a single core at 80 or 100 MHz processor, which is necessary in the scope of a vehicle implementation. In this sense, these models cannot be implemented to achieve a real-time computation loop while monitoring many cells in a real EV application.

To answer this issue, this paper presents a real-time working algorithm which allows the on-line identification of the cell model. The proposed algorithm supports the simultaneous model identification of 16 Li-ion cells and can be run with less than 500 kbytes of memory on an 80 MHz CPU. This model uses no logarithm functions, nor the computation of exponential, square roots or power functions. The proposed implementation is also entirely made with fixed-point data.

The remainder of this paper is organized as follows. Section 2 describes the BMS requests overview to design an accurate system for EV application. The proposed approach, including the algorithm is presented in Section 3. The test methodology as well as the bench test are fully depicted in Section 4. Section 5 presents the implementation and main results. Finally, Section 6 presents the main conclusions of this work

2 Overview of Battery Management System Functions

2.1 Cell voltage, current and temperature measurements

Every aspect of the electrical model presented in Fig. 1 can be modeled throughout 4 basic readings: voltage, current, temperature and a time-reference. With these four measurements, the model parameters of Fig. 1 can be estimated in real-time.

Voltage readings of individual cells comes from an analog to digital converter (ADC). Every input should be isolated from the other. Application Specific Integrated Circuits (ASICs) on the market already exists, which offer measuring features especially dedicated to Li-ion voltage readings, like built-in passive balance outputs or daisy-chainable integrated circuits [9] - [11]. String current measurement can easily be accomplished by using a Hall-effect transducer in series with the cell string. As most studies suggest [12], [13], temperature variations between adjacent cells is low enough to assume homogenous cell temperature under normal operation. Thus, in the proposed implementation, temperature is measured for a group of cells (generally between 4 and 10). The time reference is easily assured by the real-time clock and calendar (RTCC) peripheral built-in in the used controller.

2.2 R_{in} estimation

Various methods have been proposed for measuring or estimating the internal resistance (R_{in}) of a Li-on cell. In this work, R_{in} is taken as the equivalent resistor placed in the voltage-source-resistor classic electrical model which would produce a given voltage drop for a given current demand. This R_{in} can also be split into two distinct contributions: the ohmic resistance (which is constant over every frequency (denoted R_Ω) and

the polarization impedance which varies with the variation of the current flow (denoted Z_{pol}). This polarization impedance is made with a succession of RC circuits, denoted R_{pol} and C_{pol}. Each RC circuits will have distinct time constant. Some of those will have a fast response time constant, with $\tau \approx 1$ ms, and some will have a slow response time constant, with $\tau \approx 1$ s.

When implementing a resistance measurement algorithm on a real-time controller, R_{in} is estimated every couple of seconds due to the high number of cells. Thus the fast response C_{pol} part will always be completely charged, making its associated R_{pol} fully effective to the voltage drop. The R_Ω will be a representation of (R_Ω + R_{pol}) for the fast response parts of Z_{pol} and R_{pol} will only be a representation of slow response parts.

One method used to get the R_{in} estimation while using very low computation time is given in (1). This estimation can be run many times during a current pulse, enabling to separate R_Ω from R_{pol}, as shown in Fig. 2 [14].

$$R_{in} \approx \frac{\Delta V}{\Delta I} \tag{1}$$

where ΔV, in volts, is the voltage drop, ΔI, in ampere, is the current drop and R_{in}, in Ohms, is the estimated internal resistance. The same equation apply for positive pulse (i.e. in charge mode).

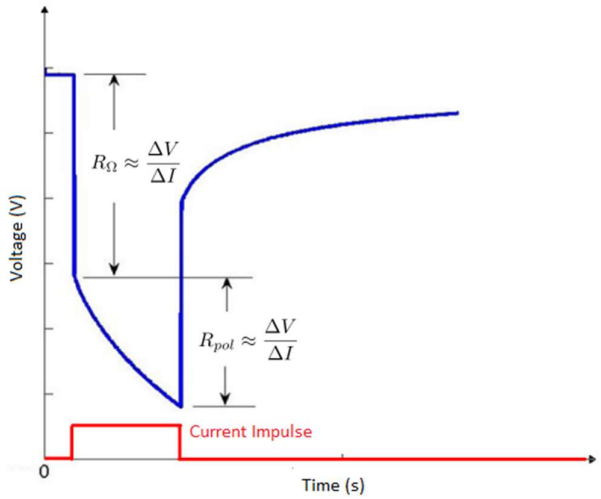

Figure 2: Estimation of R_{in}, R_Ω and R_{pol} [14]

It is known that R_{in} will be influenced by the cell temperature, current magnitude, SOC and aging [2]. The BMS software should implemented a method to differentiate a R_{in} variation based of each of those factors, and treat threat, if any, accordingly.

A good R_{in} estimation is important for EV application as it define the available power (*P*), heat generation (losses *L*) and the cell efficiency (*Eff*), as described in (2). EV designers will often change their regenerative braking strategies in order to maximize efficiency or to limit losses. The same idea goes for hybrid vehicle, the internal combustion engine will be used with the electric motor to achieve the highest efficiency for the task. If the R_{in} is not correctly estimated, those strategies may miss the optimal point.

$$\begin{aligned} P &= \left(OCV - (I * R_{in})\right) * II \\ Loss &= I^2 * R_{in} \\ Eff &= \frac{P}{P + Loss} \end{aligned} \tag{2}$$

Where *OCV* is the open circuit voltage in volts, *I* is the current in ampere, *P* is the developed power in watts, *Loss* is the heat generated in watt and *Eff* is the overall efficiency of the cell.

2.3 SOC estimation

A useful information to the driver is the amount of energy available in the battery pack. A percentage of the remaining energy in relation to its maximum value is defined as the SOC of a Li-ion cell. A minimum SOC value is targeted for every cell and also for the overall battery pack (so the driver will not force a cell into an over-discharged state).

SOC estimation can be carried out by determination of the Ampere-hour (Ah) drained from the cells. depth of discharge (DOD) can also be used. An important difference between the SOC and the DOD representation concerns the various SOC values in a string for a given DOD. As a given current value flows in a string of cells, where each cell as a distinct capacity, the DOD for a series of cell will be the same, but each will have a different SOC. DOD will also take in account the relative efficiency of the cell with temperature and current demands [8], [15]. These efficiency correction tables come from experimental values. DOD and SOC of each cells is acquired with (3) and (4).

$$\Delta DOD = \int_0^t k1[i(t)] * k2[T(t)] * I(t) * dt \tag{3}$$

$$SOC = \frac{Capacity - DOD}{Capacity} * 100\,\% \tag{4}$$

where ΔDOD, in Ah, is the increase of the depth of discharge, *k1* is the efficiency correction factor for the given current value, k2 is the efficiency correction factor given for this temperature, *I*, in A, is the current amplitude.

2.4 Capacity measurement

In order to monitor the fading of the cell capacity with time, the BMS requires a calibration discharge once in a while. The calibration discharge process involves a complete discharge of the cell energy and a monitored recharge. There is no mandatory frequency but a monthly capacity check is proposed here. As the vehicle cannot be driven during such a calibration process, it is necessary that the vehicle computer selects the appropriate time for automated diagnostics of duration of about 3 hours, where the vehicle is out of duty. Night time is probably the most suitable period of time for this task.

The function of monthly capacity estimation is actually not implemented in the EVs actually on the market. However, in the proposed BMS function breakdown, it is proposed that the capacity self-measurement be implemented. The measurement of capacity is proposed as follows:

1) Full recharge and full equalization of the battery pack;
2) 1 C constant discharge, with all DOD being monitored, until one of the cells reaches the end of discharge voltage;
3) Passive balancing of every cell until each cell reaches the end of discharge voltage;
4) The time required to empty each cell (converted in Ah) is added to the DOD of item #2, this final DOD represent the capacity of the cell;
5) Calibration is terminated with a full charge and full equalization of the battery pack.

2.5 SOH estimation

As the cell ages, its ability to store and deliver energy will fade. This is caused by the loss of reagents in the cells electrodes through irreversible and unwanted reactions in the cell. Those unwanted reactions take place normally in the cell at a normal pace through the cell lifetime, but may be quickly accelerated if the cell steps out of its safe operating area.

Generally, the loss of reagents will reduce the amount of storable energy (i.e. the capacity) or the ability to deliver this energy quickly (i.e. the R_{in}). Thus, the state of health (SOH) of a cell or of a battery pack will reflect a percentage of those performances by comparison with a brand new cell [16]. Firstly, a capacity fade threshold can be established for minimum drivable range for the electric vehicle. Secondly, the heat evacuation capability based on the R_{in} at full power will be a concern, where a maximum R_{in} value may be established as a limit parameter for the EV. A general replacement threshold for performance is suggested at 80 % of initial capacity and 200 % of initial R_{in}. A 100 % SOH cell will act as a brand new cell and a 0 %

will not deliver the designed performance (or will produce too much heat to do so). The SOH can be expressed as:

$$SOH = \min \begin{cases} \left(\frac{R_{max} - R_t}{R_{max} - R_0}\right) * 100\ \% \\ \left(\frac{C_t - C_{min}}{C_0 - C_{min}}\right) * 100\ \% \end{cases} \quad (5)$$

where C_0 is the initial capacity in Ah, C_{min} is the minimum acceptable capacity in Ah, C_t is the current capacity, R_0 is the initial R_{in}, R_{max} is the maximum acceptable R_{in} and R_t the current R_{in}.

To prevent the SOH to drop quickly if the R_{in} rise with one strong current demand, the R_t come from an average over a few hours.

2.6 Leakage estimation

Any cell will be affected by self-discharge, that is SOC decreasing naturally with time, even if the cell is not used. This leakage comes from the non-perfect isolation in the electrolyte between the two electrodes. Even though this leakage current is very small, it differs from one cell to another, and will drift with temperature changes or SOH evolution. This will result in small variations in the DOD of every cell in a battery pack.

Generally, this phenomenon is so slow that regular equalization through balancing will cover up the effects. It is one of the essential functions of the BMS to provide equalization.

2.7 Balancing of charges

As seen with past sections, every cell will show different capacity and different leakage current which will result in small variations in the SOC through the entire battery pack. If not corrected, the battery will be limited in its use as the higher SOC will limit the charge (to prevent this cell from overcharging) and the lower SOC will limit the discharge (to prevent this cell from over discharging). Each percent of the SOC between these two extremes will be an unusable stored energy, and will decrease the battery pack performance.

A simple strategy to limit this phenomenon is to balance the cells, which means to bring back all SOC to a common point. For example, passive balancing is used for bleeding the excess energy of cells with a higher SOC at the end of charge until all cells reach 100 % at the same moment in time (i.e. their maximum Voltage in the SOA where the cell is considered as full). Active balancing is another, more complex, way of balancing charges where instead of losing exceeding charges in heat, the BMS move charge from one cell to another (or from/to a group of cells) through converters [2], [3], [17].

For this research, passive balancing was implemented with MOSFETs and 47 Ω resistors.

3 Proposed Methodology for the monitoring of R_{in}

Measuring the internal resistance of hundreds of cells simultaneously and recording the evolutions of each resistance over time with low-cost is a challenge. Having a single processor core computing the cell model repeatedly for each cell will exceed its capability if the calculation algorithm is not properly designed. Having a model too complex will require more processors for the same number of cells; or require stronger processors. Using more processors or more advanced ones for a same number of cell will make this solution more expensive and less attractive for automotive highly competitive market.

The model proposed in this paper works on a PIC32MX795F512L and can support the real-time computation of the cell parameters for at least 16 cells. The novelty of the proposed method relies on the way R_{in} is monitored. The proposed strategy uses the simple method expressed in (1), but stores the R_{in} value in such a way that they are able to build trends for each driving conditions encountered. In the long run, estimations output by this method are as accurate as the ones from the complex models, but requires less computational time and less memory usage.

In order to get relevant results, the assumption is made that the current impulse used to get R_{in} is short enough to consider the starting edge from the final edge in the same driving conditions.

3.1 Typical chronological data logging and its limitation

In previous applications, BMS will store all recorded data through chronologically, by sampling every value of R_{in} measured and storing it into memory. Every reading will be timestamped and placed one after the other in memory. So the R_{in} will be placed along its driving condition (current, temperature, SOC, etc.) in one big data structure. To provide an accurate estimation, the BMS will have to average some readings together in order to have a relevant output [3]. At some point, a large number of data will be saved in memory. These readings will eventually full the onboard RAM memory and the BMS will have to address his reading to a slower, yet bigger, memory - typically a FLASH device capable of holding a couple of gigabyte of information.

When making a R_{in} average, a BMS do not want to blindly take the latest readings, as the driving conditions and the associated R_{in} can change quickly. In order to get a good picture of the R_{in}, the BMS will have to search through its entire data log for other measures captured in a similar combination of current, temperature and SOC. This search for relevant data is somewhat random and can require thousands of unnecessary access to the memory peripheral.

Therefore, the BMS would rather know where is stored relevant data instead of knowing when it was recorded. With this approach, the chronological data logging is not the best option for EV BMS.

3.2 A new data logging method

In fact, it would better to store data based on diving condition rather than linear in time. To do so, the BMS proposed in this paper creates a five-dimension cloud in memory where each coordinates represents a R_{in} measured in a given driving condition. The relation between those coordinates and a physical 32-bit memory address is given in Fig. 3. The {Temp., SOC, I, R_{in}} combination will create a four-dimension matrix in a single file in memory. For convenience, the fifth dimension (the cell #) was made through 16 separate files in memory. The cell number could have been added in the matrix segmentation shown in Fig. 3, but experience shown that working with separate files for each cells was easier [3].

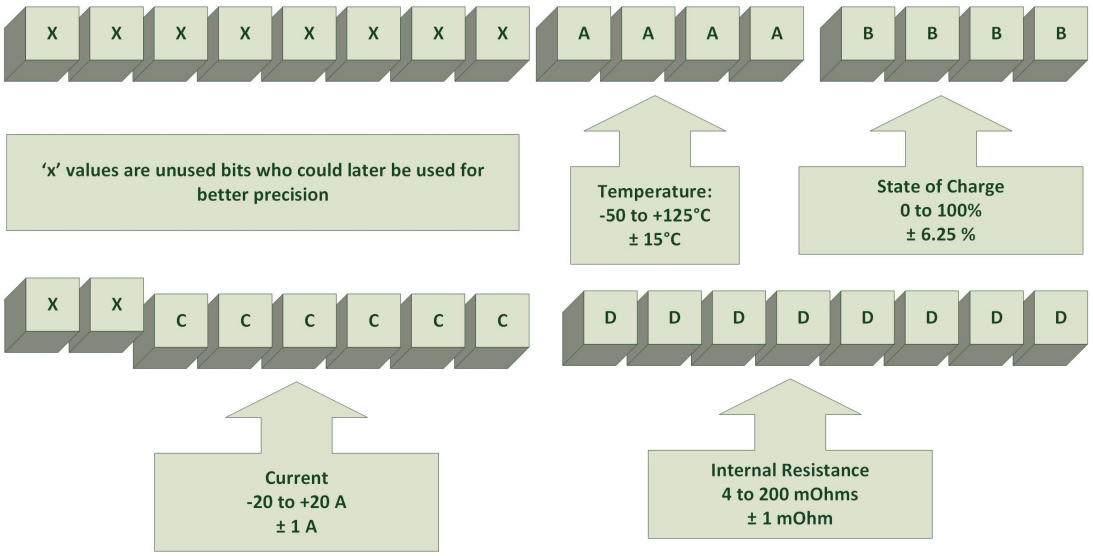

Figure 3 : 32-bit address to coordinates conversion table

Every time a R_{in} is measured in a given driving condition, the memory space associated with those coordinates is increased by one. Upon recovering, the value stored in memory represent the number of time this R_{in} at these driving condition was measured; the higher the number, the more weight it will get in the following calculations.

The main advantage of using this storage method is that the BMS doesn't need to search its values through time. It can directly access the relevant section in the cloud, leaving the irrelevant part untouched. The number of requests on the data bus between the CPU and the memory, being one of the slowest section of a BMS, is cut down to a minimum.

During run-time, the BMS will want to correlates its actual reading with past values. The current combination of {Temp, SOC, Current, R_{in}} will be the starting point. The BMS will gather the count stored within this memory slot. Then, the BMS will look on both sides of each axis and gather a set of measures all close to the starting point. This set will be called the group $\mathbb{E}$. The farther the measure is from the starting point (i.e. the center of $\mathbb{E}$), the less relevant it is for the BMS, so a weight value will be added to represent the distance between a recovered measure and the center of $\mathbb{E}$.

Once every data is recovered in memory, the BMS can make a solid R_{in} estimation with the multi-dimensional moving average presented in (6) [3].

$$R_{in\ filtered} = \frac{\sum_{\forall k \in \mathbb{E}} (R_{in(k)} * Count_{(k)} * Weight_{(k)})}{\sum_{\forall k \in \mathbb{E}} (Count_{(k)} * Weight_{(k)})} \quad (6)$$

Note should be taken that using this method removes any relation between measures and time. In order to forget old and less relevant values, the BMS shall decrease some count value to all memory slots the cloud matrix when the EV is not running. This decay allows the R_{in} to evolve on a long period of time – as it's expect to rise through the passing years.

3.3 Benchmarking the cells

R_{in} from this model will be compared with a precise, trusted and non-real-time method. If both data correlates, it means that the used model is correct and the R_{in} data estimated in real-time by the BMS is relevant.

An electronic load was used with an oscilloscope to generate trusted current pulses and precise voltage recordings in order to benchmark the cells. The recordings were analyzed with a MATLAB script to extract cells values. The baseline data is shown in Table 1.

Table 1: Benchmarked values of the 16 cells

Cell	R_{Ω} (mΩ)	R_{pol} (mΩ)	R_{in} (mΩ)	Initial Capacity (Ah)
1	21.7	2.7	24.4	2.26
2	18.0	4.3	22.3	2.21
3	21.7	2.5	24.2	2.27
4	22.7	2.4	25.1	2.27
5	16.0	3.7	19.7	2.27
6	14.5	4.5	19.0	2.21
7	17.2	4.5	21.7	2.26
8	18.4	3.5	21.9	2.25
9	16.3	4.3	20.6	2.26
10	17.2	4.1	21.3	2.09
11	14.0	4.0	18.0	2.26
12	14.4	4.1	18.5	2.26
13	13.9	4.1	18.0	2.26
14	16.7	4.7	21.4	2.25
15	17.7	4.8	22.5	2.17
16	12.5	4.5	17.0	2.27

4 Test Methodology

In order to test the new data logging method, a fully functional BMS has been made. Following every requirement mentioned in section 2, the BMS was implemented on a PIC32MX795F512L of Microchip Technologies (for computation and time reference), three BQ76PL536 of Texas instrument (for voltage and temperature readings) and a Hall-Effect sensor for a current input. The battery pack was made of 16 $LiFePO_4$ cells. Fig. 4 shows a picture of the resulting bench test.

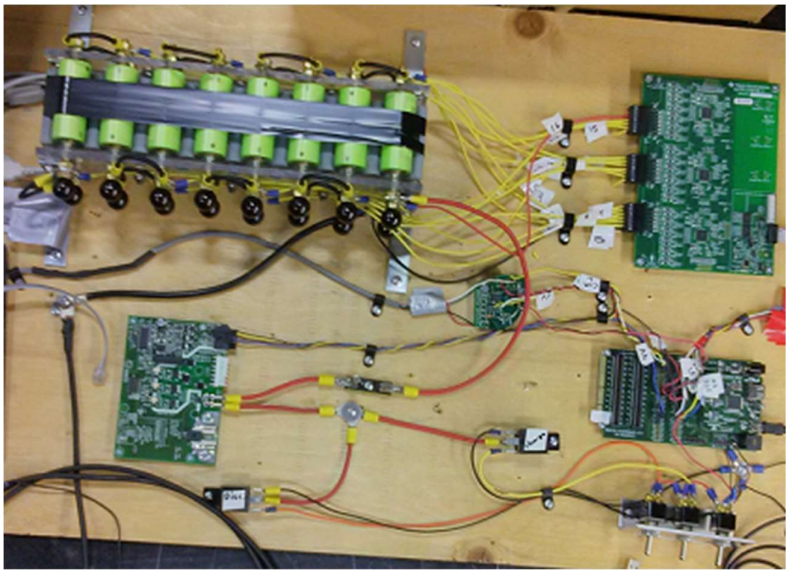

Figure 4: The bench test

A programmable electronic load and a programmable power supply were placed in a circuit with this battery pack. These two device where electronically controlled to produce current patterns which would occur in a real driving cycle. Those current curves come from a *World-wide Motorcycle Emissions Test Cycle* (WTMC) driving cycle applied to a three-wheel recreational motorcycle [16], [18], [19].

The current curves for one WTMC cycle is shown in Fig. 5. Other current curves were used, like step of 1 C, 2 C, 4 C, 6 C and 8 C, but are not shown.

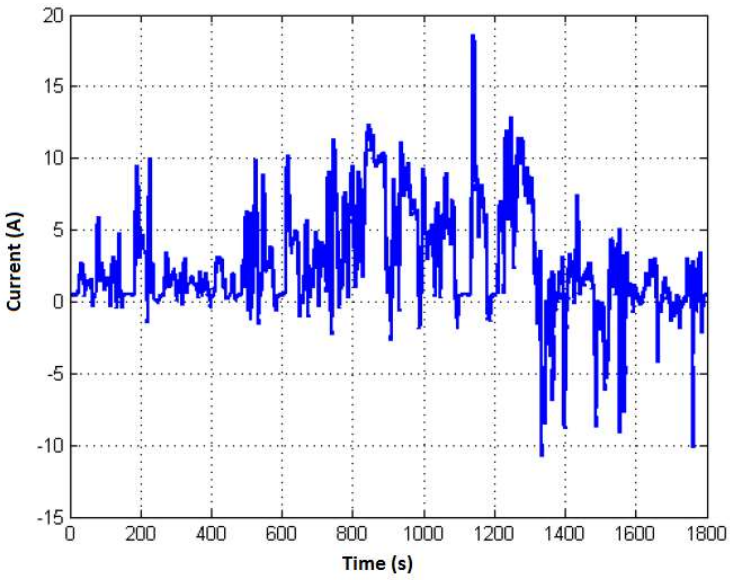

Figure 5 : Current amplitude under WMTC driving cycle

5 Results

First thing to be tested with the BMS is the cell voltage discrepancies. Fig. 6 shows that the voltage of each cell is individually measured along with the line current.

With these individual values, the BMS is able to acquire many R_{in} estimation through a driving cycle, as seen in Fig. 7. From this figure, two things can be clearly seen. First, the R_{in} is not constant from one cell to the

other in the same row. Secondly, the R_{in} of each cell rises when the current increases. Based on that second observation, all values where gathered and averaged to form a R_{in} versus current graph, shown in Fig. 8. With this figure, the real-time BMS indicates that the R_{in} is higher with higher current demands. So a BMS cannot take a single R_{in} measurement, memorize such a single value and keep it for each subsequent calculation. This R_{in} vs I relation must be kept if the BMS wants to make accurate estimations.

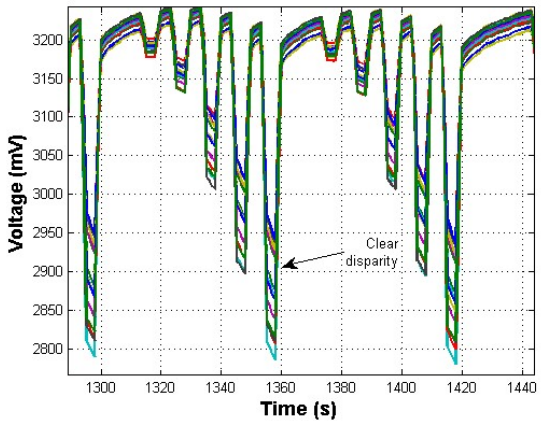

Figure 6: BMS voltage readings

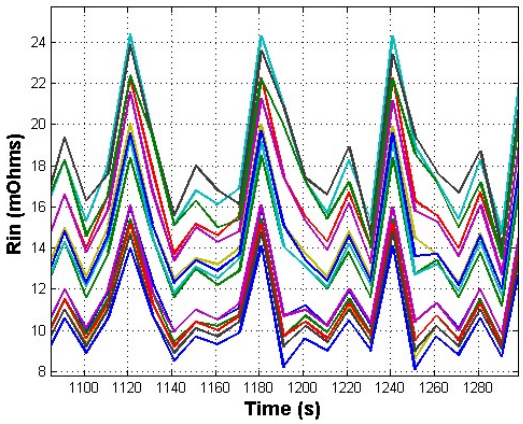

Figure 7: R_{in} Measurement

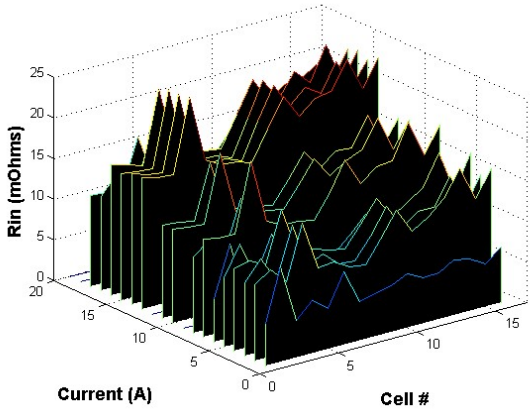

Figure 8: R_{in} versus Current comparison

With those readings, it was observed that the same current pulse does not produce equal voltage drops for the same cell, resulting in different R_{in} estimations. This leads to another test where each recorded R_{in} value was counted and expressed as a function of the current demand. A few cells, like cell #11 in Fig. 9, showed very large distribution, while other cells, like cell #13 in Fig. 10, showed very narrow distribution.

Another interesting observation is that R_{in} readings where not constant over the whole SOC range. As seen in Fig. 11, R_{in} is higher near 100 % of SOC and near 0 %.

Since R_{in} estimations changed from one measuring time to the other but not in a uniform manner, it is important to consider the average behavior of the battery pack. The following table expresses the mean value of the 16 cells for their minimum value, mean value and maximum value. Through all measured data, a σ was calculated to express the level of variation, the σ shown in Table 2 represent the mean value of all σ of the 16 cells.

Table 2: Mean value of R_{in} variations of 16 Li-ion cells

Current	R_{in} min (mΩ)	R_{in} mean (mΩ)	R_{in} max (mΩ)	σ (mΩ)
1 C	10.1	13.05	23.2	2.12
2 C	10.4	13.25	21.0	1.87
4 C	10.4	14.30	21.2	2.59
6 C	10.6	14.06	21.4	2.60
8 C	16.4	18.55	21.1	1.09

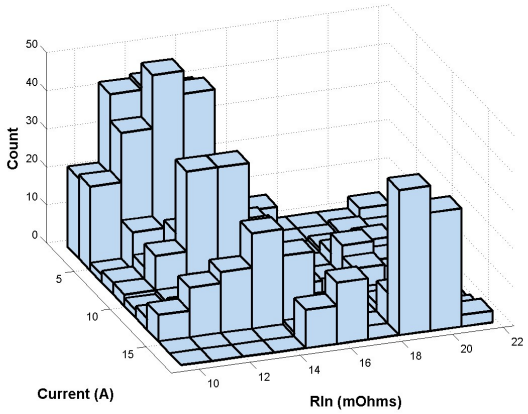

Figure 9: Cell #11 R_{in} count versus Current

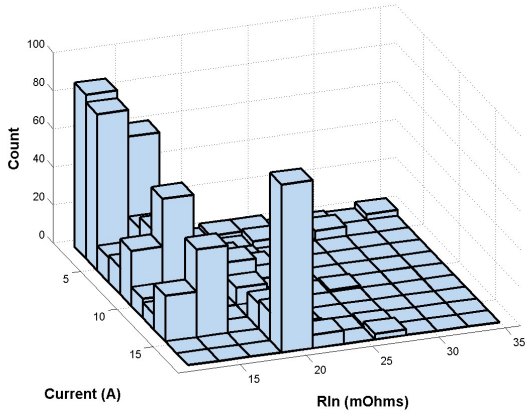

Figure 10: Cell #13 R_{in} count versus Current

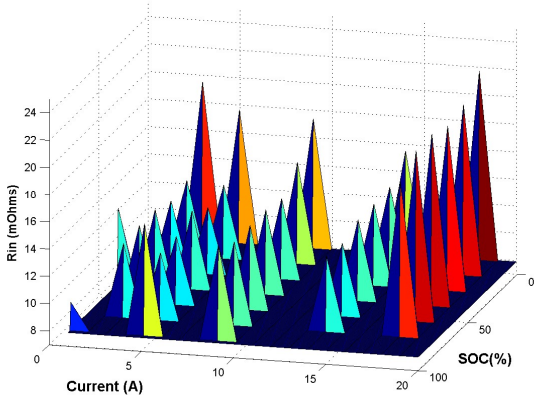

Figure 11: R_{in} versus Current and SOC comparison

It is worth noticing that the recorded R_{in} is always higher than the R_{in} value provided in the manufacturer datasheet. This said, special care must be taken when designing a battery pack (especially for range or cooling requirements) as the real usable power will be lower than announced. For example, a 10 mΩ cell under 8 C current (18.4 A) should develop 3.39 W of heat. From those results, #4 at 8 C shown a mean R_{in} value of 24.49 mΩ, which would actually develop 8.3 W of heat. In the same way, if available power and efficiency is expressed as (2), this cell would offer 52.4 W and 86.3 % instead of 57.3 W and 94.4 % at 8 C. This observation shows that cooling design must not be based solely from the manufacturer's predicted R_{in}.

6 Conclusions

This papers presents a clear model for monitoring Li-ion cells and shows basic BMS functionality. The advanced and complex models currently offered allow to fully understand cells behavior, but when applied

to a multitude of cells of an EV battery pack, it cannot be mount on small automotive embedded processor. In order to monitor >10 cells, the model used must sacrifice some accuracy to maintain real-time monitoring.

The proposed model on this paper is less precise than advanced model, but it is able to achieve relevant performances for EV applications. The BMS software runs on an 80 MHz, single processor, and is able to monitor 16 cells in real-time. One novelty comes from the R_{in} readings storage and recover method. Having a fast response way to store and recover data in memory enable the real-time model to keep the relation between R_{in} and the driving conditions.

Future work will quantify benefits of this method over traditional chronological data logging and will present some advanced BMS algorithm to enhance Li-ion life span.

References

[1] P. A. Cassani and S. S. Williamson, "Significance of battery cell equalization and monitoring for practical commercialization of plug-in hybrid electric vehicles," in Applied Power Electronics Conference and Exposition, 2009. APEC 2009. Twenty-Fourth Annual IEEE, 2009, pp. 465–471, iD: 1.

[2] D. Andrea, Battery Management Systems for Large Lithium-Ion Battery Packs, 1st ed. Artech Hous Publishers, 2011.

[3] A. Tessier, "*Bloc batterie li-ion pour véhicules électriques: méthode de classement novatrice en temps réel des paramètres électriques des cellules*," Master's thesis, Université de Sherbrooke, 2015.

[4] O. Tremblay and L.-A. Dessaint, "Experimental validation of a battery dynamic model for EV applications," World Electric Vehicle Journal, vol. 3, no. 1, pp. 1–10, 2009.

[5] Y. Hu and S. Yurkovich, "Linear parameter varying battery model identification using subspace methods," Journal of Power Sources, vol. 196, no. 5, pp. 2913–2923, 3/1 2011.

[6] F. Sun, X. Hu, Y. Zou, and S. Li, "Adaptive unscented Kalman filtering for state of charge estimation of a lithium-ion battery for electric vehicles," Energy, vol. 36, no. 5, pp. 3531–3540, 2011.

[7] N. Watrin, B. Blunier, and A. Miraoui, "Review of adaptive systems for lithium batteries state-of-charge and state-of-health estimation," in Transportation Electrification Conference and Expo (ITEC), 2012 IEEE. IEEE, 2012, pp. 1–6.

[8] V. R. Tannahill, D. Sutanto, K. M. Muttaqi, and M. A. Masrur, "Future vision for reduction of range anxiety by using an improved state of charge estimation algorithm for electric vehicle batteries implemented with low-cost microcontrollers," IET Electrical Systems in Transportation, 2014.

[9] BQ76PL536 datasheet. Texas Instrument, http://www.ti.com/product/bq76pl536/description, accessed on 2015-11-01

[10] LTC6804 datasheet. Linear Technologies, http://cds.linear.com/docs/en/datasheet/680412fb.pdf, accessed on 2015-11-01

[11] MAX11068 datasheet. Maxim Integrated, http://www.maximintegrated.com/en/products/power/battery-management/MAX11068.html, accessed on 2015-11-01

[12] A. Landry-Blais, "Modélisation du système de gestion thermique d'un véhicule hybride," Master's thesis, Université de Sherbrooke, 2014.

[13] G. Damblanc, S. Hartridge, R. Spotnitz, and K. Imaichi, "Validation of a new simulation tool for the analysis of electrochemical and thermal performance of lithium ion batteries." JSAE Annual Congress, p. 6, 2011.

[14] X. Wei, B. Zhu, and W. Xu, "Internal resistance identification in vehicle power lithium-ion battery and application in lifetime evaluation," in Measuring Technology and Mechatronics Automation, 2009. ICMTMA '09. International Conference on, vol. 3, 2009, pp. 388–392, iD: 1.

[15] K. P. Angarita, "*Modélisation électrique et analyse d'une cellule lithium*," Master's thesis, Université de Sherbrooke, 2012.

[16] J. Nadeau, M. Dubois, A. Desrochers, and N. Denis, "Ageing estimation of lithium-ion batteries applied to a three-wheel phev roadster," in Vehicle Power and Propulsion Conference (VPPC), 2013 IEEE. IEEE, 2013, pp. 1–6.

[17] J. Cao, N. Schofield, and A. Emadi, "Battery balancing methods: A comprehensive review," in Vehicle Power and Propulsion Conference, 2008. VPPC'08. IEEE, 2008, pp. 1–6, iD: 1.

[18] N. Denis, M. R. Dubois, K. A. Gil, T. Driant, and A. Desrochers, “Range prediction for a three-wheel plug-in hybrid electric vehicle,” in Transportation Electrification Conference and Expo (ITEC), 2012 IEEE. IEEE, 2012, pp. 1–6.

[19] J. P. Trovao, M. R. Dubois, M. A. Roux, E. Menard and A. Desrochers, "Battery and SuperCapacitor Hybridization for a Pure Electric Three-Wheel Roadster," in IEEE Vehicle Power and Propulsion Conference (VPPC), Montreal, QC, 2015, pp. 1-6.